Temperature dependence of the magnetic-moment distribution around impurities in iron*

H. R. Child and J. W. Cable
Solid State Division, Oak Ridge National Laboratory, Oak Ridge, Tennessee 37830
(Received 23 July 1975)

We have made neutron diffuse-scattering measurements of the magnetic-moment distribution around impurities in Fe as a function of temperature in an attempt to obtain information regarding the range of the exchange interactions. The measurements were made on Fe-based alloys containing 2–3 at.% of Si, Ge, Ti, V, Mn, Co, and Ni at temperatures ranging from 300 to 800 K. The *Fe*Ti, *Fe*V, *Fe*Co, and *Fe*Ni cross sections show very little temperature dependence while the *Fe*Si, *Fe*Ge, and *Fe*Mn show pronounced thermal effects. This observation can be explained by a nearest-neighbor molecular-field model by assuming that the impurity-host to host-host exchange ratio is near unity for Ti, V, Co, and Ni impurities and small for Mn impurities, an assumption that is supported by T_C-vs-c data. Furthermore, the observed temperature dependences for *Fe*Si, *Fe*Ge, and *Fe*Mn are described reasonably well by this model provided that the low-temperature moment distributions are included in the calculation. We conclude that the magnetic moment of an Fe atom depends on its local chemical environment and on its local magnetic environment. We attribute the latter to nearest-neighbor exchange interactions.

INTRODUCTION

The temperature dependence of the magnetic-moment distribution at and around impurity atoms in ferromagnetic hosts provides indirect information regarding the range of the exchange interactions. There has been a great deal of activity in this area since the observation[1] of an anomalous temperature dependence of the Mn hyperfine field in an *Fe*Mn alloy. These results have been explained[2-4] by a nearest-neighbor molecular-field model with a weakly coupled Mn moment. This model also predicts[5-9] a stronger temperature dependence for the host moments surrounding the impurity than for the pure host, and the calculated behavior is in qualitative agreement with hyperfine-field data from Mössbauer measurements.[9,10] In the other limit, the purely itinerant model, the magnetic response of an electron gas to the charge or moment perturbation of an impurity is also temperature dependent.[11,12] Thus, with appropriate parametrization, either a short-range local-moment model or a long-range itinerant model can be used to describe a temperature-dependent moment distribution. The best model and the best parameters have not yet been established.

Most of the experimental studies to date have been carried out either by NMR or Mössbauer techniques. Although these are more sensitive to moment disturbances than neutron scattering methods, there remains some uncertainty both in the assignment of the observed shifts to the proper local environments and in the appropriate conduction-electron and core-polarization contributions to the hyperfine fields. We have therefore undertaken a neutron study of the temperature dependence of the moment distributions in a few Fe-based alloys. This is the first systematic study of this type by the neutron method.

THEORY

The theory of magnetic-diffuse scattering of unpolarized neutrons from ferromagnetic alloys has been elegantly described by Marshall,[13] whose formalism we adopt in this paper. The magnetic-disorder cross section is given by

$$\frac{d\sigma}{d\Omega}(K) = c(1-c)\left(\frac{e^2\gamma}{2mc^2}\right)^2 q^2 f(K)^2 M(K)^2, \tag{1}$$

in which $K = 4\pi \sin\theta/\lambda$, $f(K)$ is the magnetic form factor, c is the fractional impurity content, $e^2\gamma/2mc^2$ is a constant, and q^2 is a known function of the angle between the scattering vector and the sample magnetization. The cross section therefore determines $|M(K)|$, the Fourier transform of the magnetic-moment disturbance caused by the impurity. This transform is given by

$$M(K) = \mu_i - \mu_h + \sum_j g(R_j) e^{i\vec{K}\cdot\vec{R}_j}, \tag{2}$$

in which $g(R_j)$ is the magnetic disturbance produced at a host atom by an impurity atom at R_j.

Essentially all of the previous neutron studies of this type were carried out at low T/T_C. Since both the local and itinerant models predict a temperature dependence for $g(R_j)$, one expects a temperature dependent $M(K)$, or cross section. A realistic itinerant model has not yet been treated, but Lovesey and Marshall[5] and Lovesey[6,7] have calculated this dependence for the molecular-field model and find that large effects are possible. In

the case of a nonmagnetic impurity, the moment on the nearest neighbor of the impurity finds itself in a weaker molecular field than more distant neighbors. At low T/T_C this moment is fully aligned, but with increasing temperature, assumes a lower magnetization than the pure material. This, in turn, reduces the molecular field and magnetization of the next-neighbor shell, etc., to successive shells. The net result is a moment defect cluster surrounding the impurity atom and increasing in magnitude and radial extent with increasing T/T_C. A similar effect is calculated for magnetic impurities except that the moment disturbance can be either positive or negative depending on the ratio of the impurity-host to host-host exchange. We have used the Lovesey and Marshall formalism to calculate the moment deviations and cross sections as a function of T/T_C. The calculation is based on a nearest-neighbor exchange interaction, isolated impurities, and includes the moment deviations out to eight neighbor shells. It also allows phenomenologically for moment perturbations at low temperatures. Thus, we write the relative magnetization at distance R from the impurity as

$$\sigma_R = B_S\left(\sum_\rho \frac{J\sigma_{R+\rho}}{kT}\right), \tag{3}$$

in which the summation is over nearest neighbors. The relative moment deviations λ_R are defined as

$$\lambda_R = \sigma_R - \sigma, \tag{4}$$

where σ is the relative magnetization of the pure host. The resultant coupled transcendental equations are then solved by computer iteration to obtain the λ_R. These are readily converted to the $\mu_i - \mu_h$ and $g(R_j)$ moment deviations in Eq. (2) from which the cross sections are calculated.

EXPERIMENT

We have observed the magnetic disorder cross section for 3-at.% Si, Ge, V, Ti, Ni, Co, and 2-at.% Mn in polycrystalline Fe for $0.3 \leq T/T_C \leq 0.8$. The samples were rectangular slabs which had been machined from quenched arc-melted ingots made from the required weights of 99.99% Fe and the impurity. Since no significant weight loss was observed, the nominal concentration was taken as the actual concentration. The slabs were mounted in a furnace in which the temperature of the sample could be controlled to better than 1% at temperatures up to about 800 °K (approximately $0.8T_C$). At each temperature, two runs were made, one with no magnetic field and one with a magnetic field sufficient to magnetically saturate the sample along the scattering vector $\vec{K}$. The difference between these runs is the magnetic scattering intensity which was converted to an absolute magnetic cross section per atom by calibration with a pure V sample.

The data were all taken at the Oak Ridge Research Reactor using a 4.43-Å neutron beam and a Borkowsky-Kopp[14] position sensitive counter which covered about 26 deg of scattering angle at each setting. Two settings were used for each run to cover the approximate range $0.1 < K < 1.4$ Å^{-1}. No Bragg scattering in possible from Fe at this wavelength, so no correction was necessary for multiple scattering or the single transmission effect. To check this latter problem the transmission of some of the samples was measured with and without an applied field and no detectable difference was observed. The transmission was found to depend on temperature, however, and this effect was included in the calibration. This change in transmission and the increase in background can be explained as an increase in the magnetic scattering associated with the increasing disorder in the z component of the moment as the temperature is raised. We will refer to this as pseudo-paramagnetic scattering.

Since the disorder cross section is proportional to $c(1-c)$, the 3-at.% concentration was of necessity a compromise between a detectable signal and the isolated impurity limit which can be theoretically treated. The position sensitive counter allowed sufficient accuracy to enable us to measure cross sections in most runs with a statistical accuracy of about ±0.6 mb, and a few cases were measured statistically to ±0.3 mb. However, there is an error in the calibration in addition to this statistical error which could shift the overall scale of the data approximately ±15%. The position sensitive counter measures the total number of neutrons scattered at a fixed scattering angle regardless of their energy. However, our minimum scattering angle is beyond the spin-wave cutoff angle of Fe even at temperatures near $0.8\,T_C$,[15] so no spin-wave intensity is included. The scattering processes which can occur at fixed scattering angle fall on a parabola in E-vs-K space near $K=0$. This parabola is quite narrow for 4.43-Å neutrons so that any inelastic scattering will be restricted to energy changes of a few meV, and the dominant contribution is from elastically scattered neutrons such as the disorder scattering.

RESULTS AND DISCUSSION

Figure 1 shows typical auxiliary measurements needed for the calibration and analysis of the runs. In Fig. 1(a), the transmission of the Fe+3-at.%-Ge sample is shown versus T/T_C. (Note that the

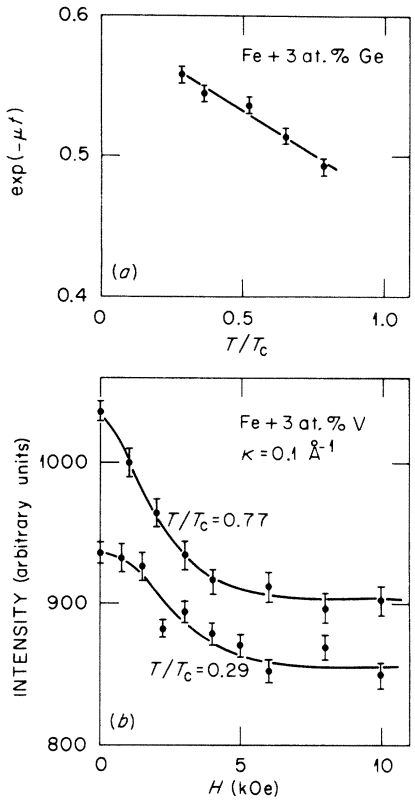

FIG. 1. (a) Transmission of *Fe* Ge sample-vs-T/T_C and (b) field dependence of small K scattering from *Fe*V.

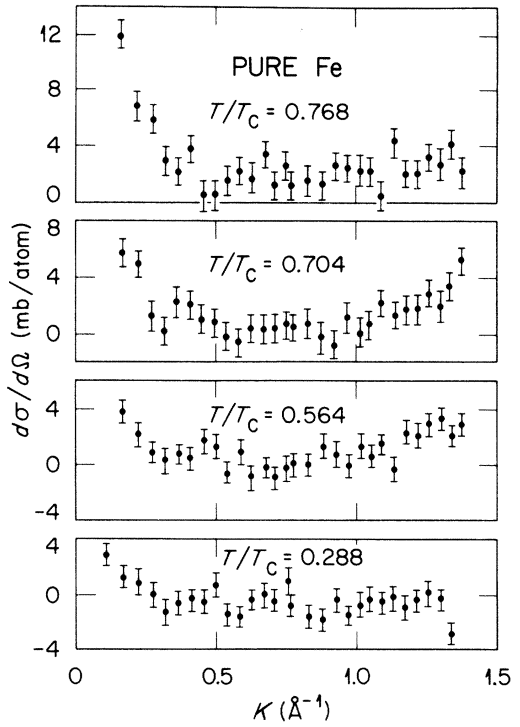

FIG. 2. Field-off minus field-on cross sections for pure Fe as a function of T/T_C.

zero of the y axis is well below the scale shown in both parts of Fig. 1.) The transmission drops slightly as T increases due to the increasing pseudoparamagnetic scattering from the sample while the corresponding decrease in Bragg scattering does not occur because we are operating beyond the Bragg cutoff. In any case, the decrease in transmission is only slightly greater than 10% and has been taken into account by a linear dependence on T/T_C as shown by the straight line in Fig. 1. The field dependence of the transmission was less than the error. Figure 1(b) shows the field dependence of the total scattering for Fe + 3-at.% V at a fixed K for two values of T/T_C. At both temperatures, the scattering is magnetically saturated, i.e., turned off for fields greater than about 7 kOe so all the field-on measurements were made with H=10 kOe applied along the scattering vector.

The magnetic diffuse scattering from an alloy contains the elastic magnetic-disorder scattering as described in the theory section and also some inelastic pseudoparamagnetic scattering. At low T/T_C, the latter is small and only weakly field dependent. However, this scattering intensity increases with increasing T/T_C and becomes sharply peaked in $\vec{q}$ and ω and field dependent as $T \to T_C$. In order to determine the importance of this scattering for this experiment, we have measured the magnetic diffuse scattering from pure Fe under the same experimental conditions. The results for various T/T_C are shown in Fig. 2 and these indicate that this contribution is small, but not negligible, at the innermost K values. Near T_C this term becomes the dominant contribution (critical scattering) so we have generally limited our measurements to $T/T_C < 0.8$.

The observed magnetic diffuse cross sections for the alloys are shown in Figs. 3–9. All of these show a sharp K dependence inside of K=0.2 to 0.3 which becomes more pronounced with increasing temperature. We attribute this to the pseudoparamagnetic term as observed in pure Fe and neglect this innermost K region in the analyses to be described later.

The present results are in good agreement with the previously reported[16,17] impurity-induced moment disturbances at room temperature. Nevertheless, a brief recapitulation of these effects will make the discussion that follows more understandable. The observed cross sections are best discussed in terms of $M(K)$, which consists of a con-

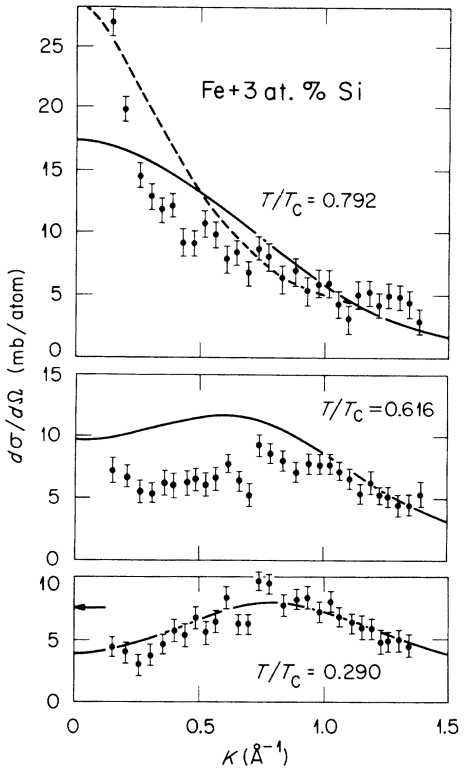

FIG. 3. Observed and calculated magnetic-disorder cross sections for *Fe*Si at selected T/T_C. The dashed curve is from Lovesey and Marshall (Ref. 5), while the solid curves represent the same formalism with inclusion of the low-T moment deviations. The arrow in the bottom section of this and the following figures indicates the $K=0$ cross section from observed $d\bar{\mu}/dc$ values.

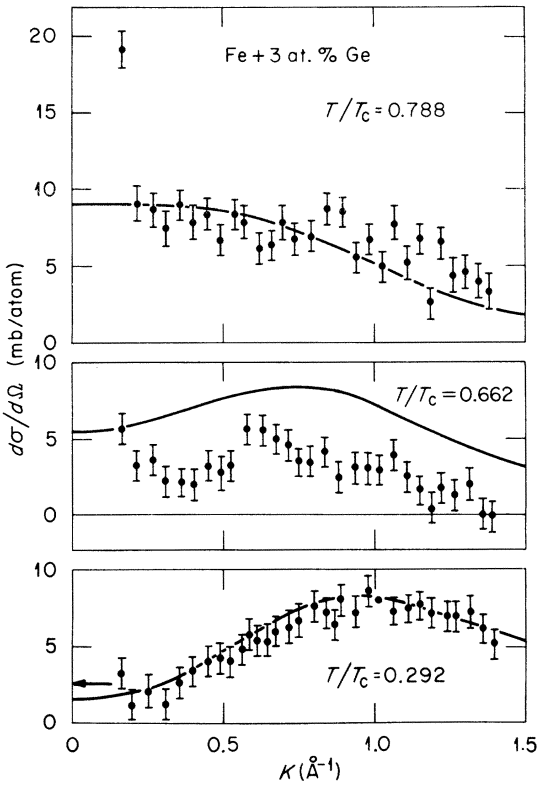

FIG. 4. Observed and calculated magnetic cross section for *Fe*Ge-vs-T/T_C. The calculated curves include the low-T moment deviations.

stant, $\mu_i - \mu_h$, plus a K-dependent term describing the host moment disturbance. In Marshall's notation,[13] this latter term is designated $G(K)=\sum g(R) \times e^{i\vec{K}\cdot\vec{R}}$. Note that $G(0)=\sum g(R)$ is the total moment disturbance in the host so that $M(0)=d\bar{\mu}/dc$. All of the room-temperature cross sections are consistent with this relationship as indicated by the arrows in Figs. 3–9 which correspond to the observed $d\bar{\mu}/dc$ values converted to cross section at $K=0$. In these Fe-based alloys $\mu_i - \mu_h$ is always negative while $G(K)$, at small K, can be either positive or negative. Three cases are represented in Figs. 3–9. For Ti, V, and Mn there is little K dependence to $M(K)$ (room temperature) so that the $\mu_i - \mu_h$ term dominates and there is little or no moment disturbance on the surrounding host atoms. For Si and Ge, $M(K)$ increases with increasing K and peaks near $K=0.8$ to 1.0. Since $\mu_i - \mu_h$ is negative, $G(K)$ is positive at small K. The shape of $G(K)$ corresponds to a positive moment-disturbance peaking about 5 Å from the impurity. For Co and Ni, $d\bar{\mu}/dc$ is positive while $\mu_i - \mu_h$ is negative so that $M(K)$ changes sign between the small K and large K regions. The cross sections indicate that this crossover occurs near $K=0.6$ in both cases. Here, the shape of $G(K)$ corresponds to $g(R_j)$'s that decrease with increasing R and extend 5 to 6 Å into the host.

At the higher temperatures, different effects are obtained for different impurities. With Ti, V, Co, and Ni impurities there is little if any, temperature dependence while for Mn, Si, and Ge large thermal effects are observed. One can rationalize this behavior, within the molecular-field framework, by assuming that in the former group the impurities have impurity-host to host-host exchange ratios near unity while in the latter group they have small exchange ratios. There is some experimental justification for this assumption. For dilute alloys, the molecular-field model yields.

$$\left(\frac{1}{T_C}\right)\left(\frac{dT_C}{dc}\right) = \epsilon^2 - 1, \tag{5}$$

where $\epsilon \equiv J_{ih}S_i/J_{hh}S_h$ is the impurity-host to host-host exchange ratio. Values[18,19] of dT_C/dc and ϵ for these alloys are given in Table I. For the transition-metal impurities, the ϵ values are in

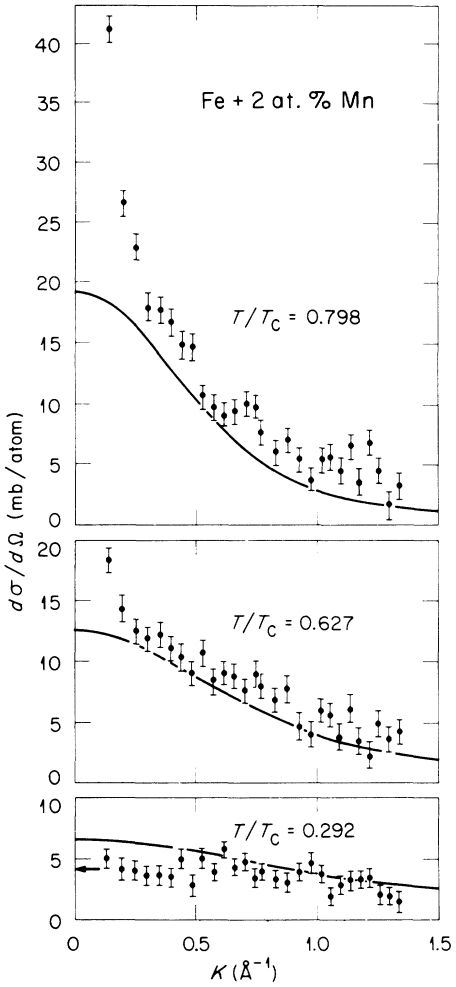

FIG. 5. Observed and calculated magnetic cross section for *Fe*Mn. The calculated curves are for $2.4\mu_B$/(Fe atom) and $1.0\mu_B$/(Mn atom) at low T and $\epsilon = 0.2$.

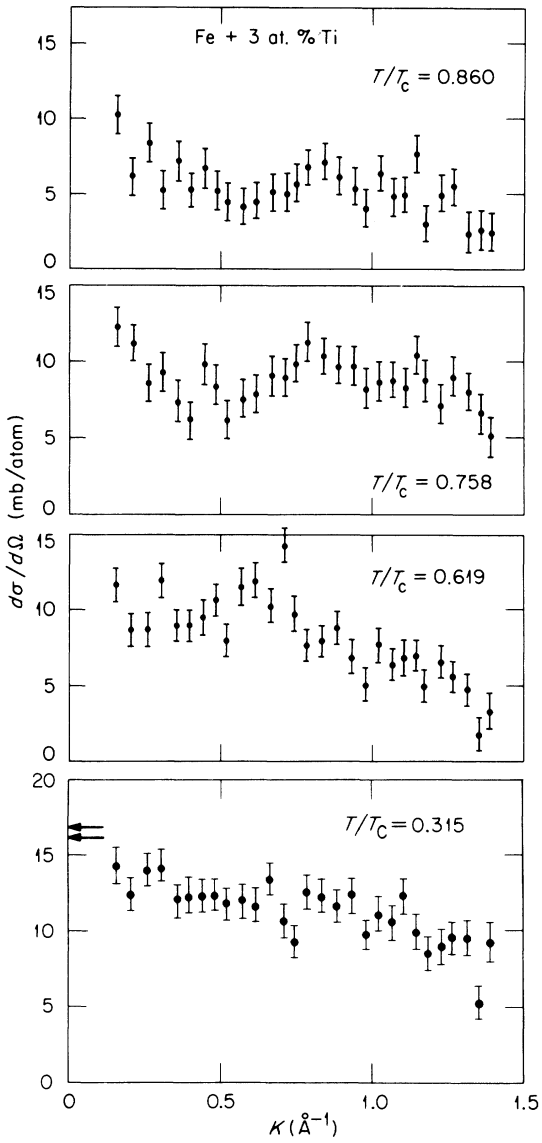

FIG. 6. Magnetic cross section of *Fe*Ti-vs-T/T_C.

qualitative accord with the neutron observations, i.e., Ti, V, Co, and Ni have $\epsilon \sim 1$ while the Mn is weakly coupled. However, the model also yields $\epsilon \sim 1$ for Si and Ge while these non-magnetic impurities should have $\epsilon = 0$.

For a more quantitative comparison, we show the calculated cross sections for the three cases with pronounced temperature effects in Figs. 3, 4, and 5. The dashed curve in Fig. 3 is taken from the calculation of Lovesey and Marshall[5] normalized to a host moment at $T=0$ of 2.4 μ_B/atom. Here, we use the neutron diffraction value[20] for the local moment rather than the magnetization value of 2.218 μ_B/atom, i.e., we assume that the negative conduction-electron polarization is spatially uniform and remains undetected in these measurements. This curve has the correct K dependence but overestimates the magnitude of the moment deviations. The results of our own calculations are given by the solid curves. Here, we have included the low-temperature moment deviations obtained by fitting the room temperature data to Eq. (2). Because of the limited spatial resolution of the measurements, we have not used the discrete $g(R_j)$'s as parameters but instead have grouped the neighboring shells in the manner used by Campbell.[21] The eight atoms in the first neighbor shell and the six atoms in the second neighbor shell are grouped and treated as 14 atoms at the weighted-average distance, R_{I}. Similarly, the third, fourth, and fifth shells are grouped into 44 atoms at R_{II} while the sixth, seventh, and eighth shells give 60 atoms at R_{III}. The fitted

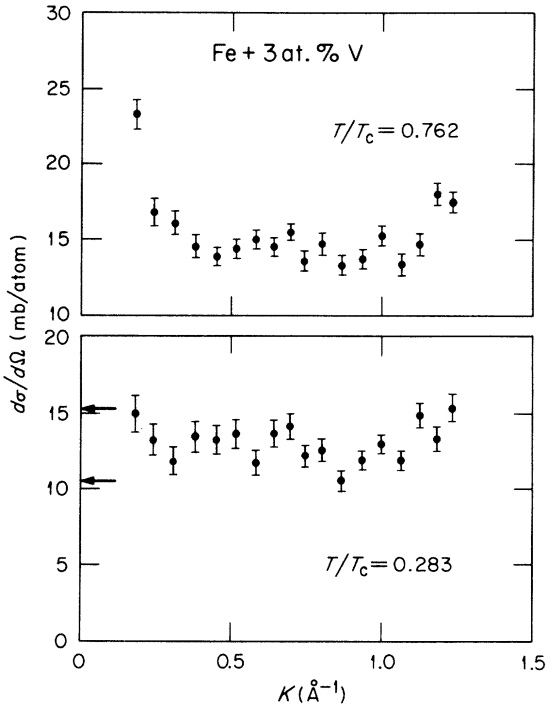

FIG. 7. Magnetic cross sections for *Fe*V. The two arrows are taken from two separate measurements of $d\bar{\mu}/dc$.

parameters $g(R_{\mathrm{I}})$ and $g(R_{\mathrm{II}})$ are given in Table II for *Fe*Si, *Fe*Ge, and *Fe*Mn. [$g(R_{\mathrm{III}})$ was insignificant in all cases.] With increasing T/T_C, the

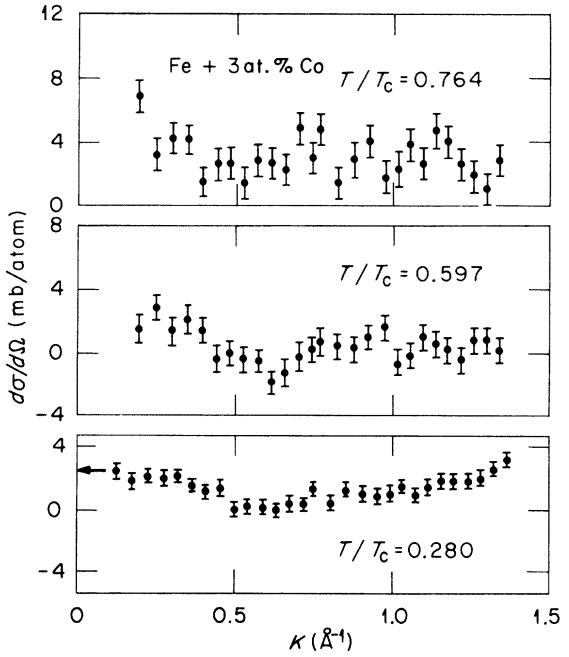

FIG. 8. Magnetic cross sections for *Fe*Co.

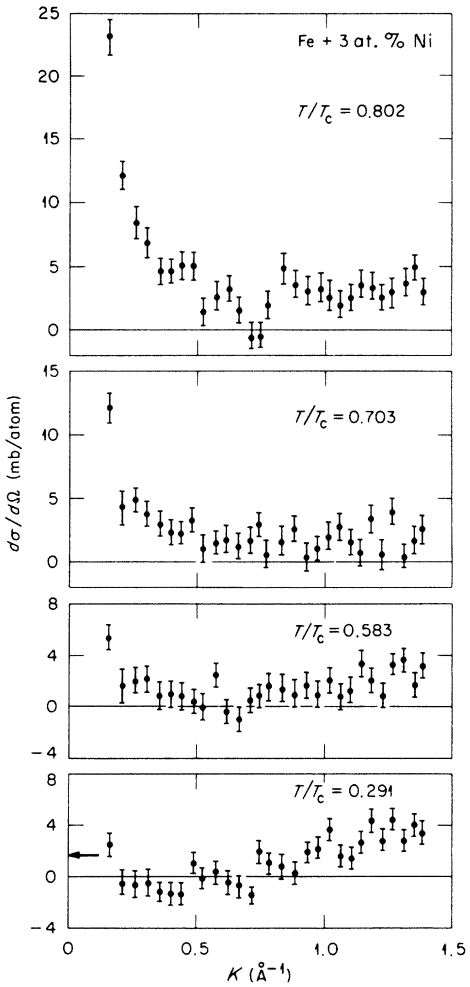

FIG. 9. Magnetic cross sections for *Fe*Ni.

$g(R)$'s become negative for these impurities but the values attained depend on the low-temperature starting point. Thus, our calculation for *Fe*Si yields a different cross section from that of Lovesey and Marshall because they omitted the low-T moment deviations. In the *Fe*Si case, the positive $g(R_{\mathrm{II}})$ retards the thermally induced

TABLE I. dT_C/dc and ϵ for Fe-based alloys.

Impurity	dT_C/dc [a]	ϵ
Ti	390	1.2
V	1110	1.4
Mn	−1150	~0
Co	1340	1.5
Ni	−360	0.8
Si	160	1.1
Ge	−200	0.9

[a] References 18 and 19.

TABLE II. Effective-moment disturbance parameters for *Fe*Si, *Fe*Ge, and *Fe*Mn at room temperature.

Impurity	$g(R_I)$	$g(R_{II})$
Si	−0.040	+0.026
Ge	+0.014	+0.028
Mn	−0.030	0

negative-moment deviations, especially in the group II shells. This effect is even more pronounced in the *Fe*Ge case for which both $g(R_I)$ and $g(R_{II})$ are positive. In the *Fe*Mn case, the calculated cross section depends on ϵ, the impurity-host to host-host exchange. Previous estimates[2,3] of $\epsilon \sim 0.2$ to 0.3 have been used to account for the temperature dependence of the Mn hyperfine field and this is consistent with our results. The calculated curves in Fig. 5 are for $\epsilon = 0.2$ and impurity and host moments of 1.0 and 2.4 μ_B, respectively, at low temperature. Clearly, the calculated cross sections correctly predict the trends of the observed temperature behavior.

The calculated and observed cross section for *Fe*Si and *Fe*Mn are different at low T/T_C but quite similar at high T/T_C. The similarity at high temperatures is presumably a consequence of the small ϵ value of *Fe*Mn so that the Mn ferromagnetic moment approaches zero in this region. The overall temperature dependence of the induced moment disturbance for these two impurities is illustrated in Fig. 10 in terms of $G(K)$. *Fe*Mn is the simpler case with a very small negative disturbance at $T/T_C = 0.292$ which becomes larger and longer ranged with increasing T/T_C. With Si impurities, $G(K)$ is positive at $T/T_C = 0.290$, passes through zero near $T/T_C = 0.616$, and then goes negative at higher T/T_C. It is interesting that the total moment change between low and high T/T_C at small K is comparable in the two cases. We note that the *Fe*Ge behavior is similar to that of *Fe*Si except that the small K region of $G(K)$ is more positive at low T/T_C and less negative at high T/T_C.

This similarity in behavior is perhaps better illustrated by conversion to real space as shown by the plots of $g(R)$-vs-R in Fig. 11. Here the data points are fitted values of $g(R_I)$, $g(R_{II})$, and $g(R_{III})$ at the indicated T/T_C values, while the solid curves are calculated by the molecular field model. In all three cases the effect of increasing temperature is to create a moment defect cluster pinned to the impurity site. These are similar in range and magnitude but differ in detail largely because of the influence of the low-temperature moment distribution.

This observation contrasts with the conclusions drawn[10] from Mössbauer data that the *Fe*Mn thermal behavior could be qualitatively described by a molecular-field model while that of *Fe*Si could not. We therefore attempt a comparison of our data with the hyperfine field data for these alloys.

The original molecular-field interpretation[2] of the Mn hyperfine field temperature dependence assumed proportionality between the local impurity moment and the hyperfine field. However, this required a moment of 2 to 3 μ_B/Mn, while the reported neutron value at room temperature was

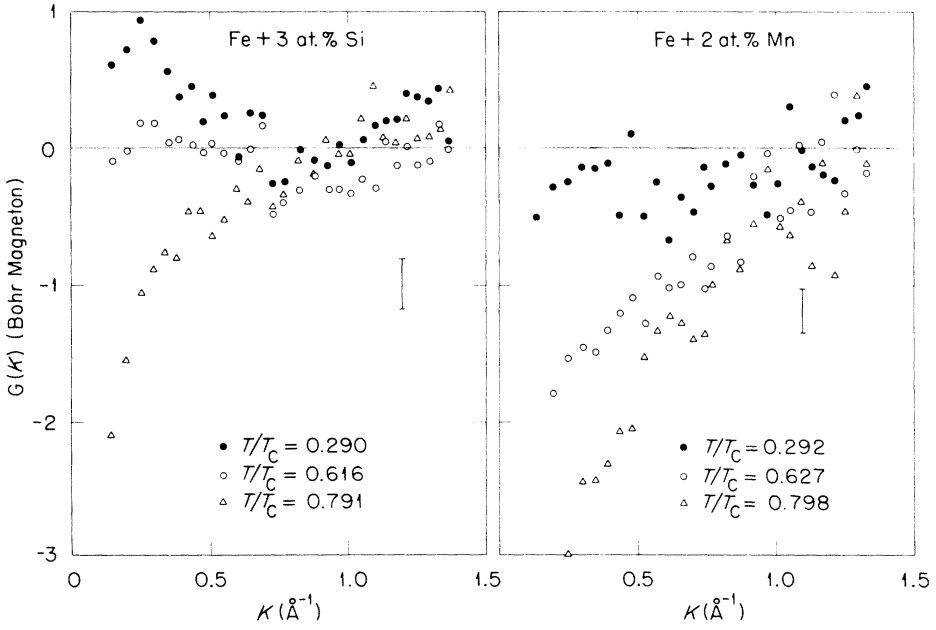

FIG. 10. Temperature dependence of $G(K)$ for *Fe*Si and *Fe*Mn. Both show negative tendencies at high T, but this is smaller for *Fe*Si because of the positive low-T deviations.

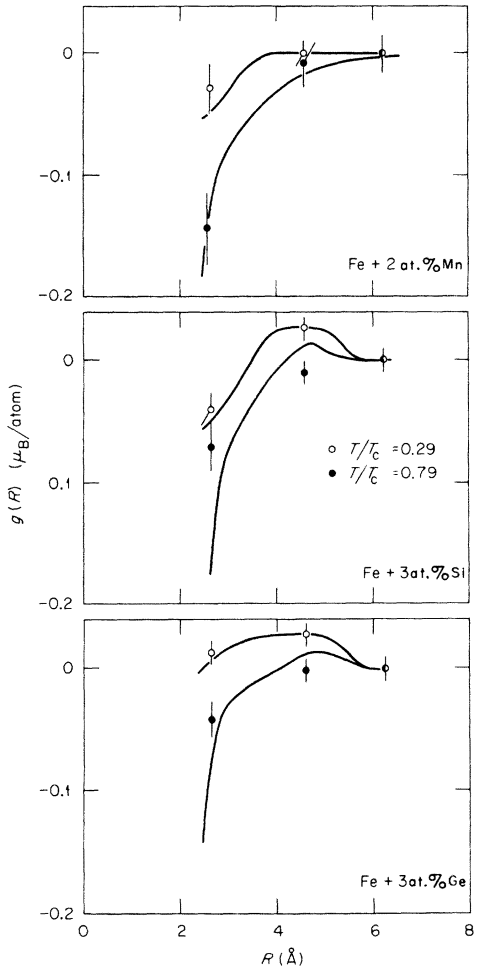

FIG. 11. Calculated and observed moment disturbance parameters for *Fe*Mn, *Fe*Si, and *Fe*Ge at $T/T_C = 0.29$ and 0.79. The calculated curves are for discrete shells while the data points are for grouped shells as described in the text.

near zero.[16] It was later shown[3-4] that the data could be fitted equally well with a small Mn moment by including in the hyperfine field a contribution from the conduction electron polarization. Nevertheless, there has remained some uncertainty in the magnitude of the Mn moment and the relative contribution of the conduction electron and core polarization contributions to the hyperfine field. At an impurity site, this is generally written as[4,22]

$$H_i = a\mu_i + b\mu_h, \tag{6}$$

in which the first term is conduction electron and core polarization at the impurity site and the last term is the conduction-electron polarization contribution from the neighbors. Estimates[4,22] of $a \sim 100$ and $b \sim 50$ kG/μ_B have been taken from the systematic variation of impurity hyperfine fields and impurity moments for 3*d* impurities in Fe. We can use this relationship to compare observed impurity hyperfine fields with the impurity moments obtained in this experiment. This comparison is given in Table III. Unfortunately, there are large errors (±0.2 to 0.3 μ_B) in the impurity moments obtained from these neutron data. Nevertheless, there is an overall consistency that tends to support Eq. (6). In particular, there is reasonable agreement between the hyperfine field and neutron results for the temperature dependence of the Mn moment. We should therefore be able to use Eq. (6) to compare the temperature dependence of $g(R_1)$ from the neutron data with the Mössbauer results[9,10,23] for the hyperfine fields at Fe atoms with impurity first neighbors. The latter is usually presented as the difference in relative hyperfine fields, $h = H(T)/H(0)$, for Fe atoms with, h_1, and without, h_0, first-neighbor impurities as a function of T/T_C. If the conduction-electron polarization is proportional to the host magnetization, then

$$h_0 - h_1 \simeq a[g(R_1, T) - g(R_1, 0)]/H_{\mathrm{hf}}^{\mathrm{Fe}}. \tag{7}$$

With $a = 100\,\mathrm{kG}/\mu_B$, $H_{\mathrm{hf}}^{\mathrm{Fe}} = 339$ kG, and $T/T_C = 0.8$, our $g(R_1)$ values give $h_0 - h_1 = 0.009$ for *Fe*Si and 0.034 for *Fe*Mn. These agree with the Mössbauer values of 0.010 to 0.018 for *Fe*Si and 0.030 to 0.040 for *Fe*Mn. The small thermal effect in *Fe*Si has been taken as an indication that long-range exchange interactions are responsible for the ferromagnetism of Fe.[10] These neutron data, however, indicate that the small thermal effect of *Fe*Si should be attributed to a modulating effect of the low-temperature moment distribution and that the observed thermal effects in Fe-based alloys can be described by a molecular-field model with nearest-neighbor interactions.

The molecular-field model does not contain low-temperature moment deviations such as those observed around Si and Ge impurities in Fe, but if

TABLE III. Impurity moments in Fe derived from hyperfine fields and neutron data.

Impurity	T/T_C	μ_i (hyperfine) [a]	μ_i (neutron)
Ti	0.315	•••	−0.4
V	0.283	−0.1	−0.9
Co	0.280	1.8	1.4
Ni	0.291	1.3	0.8
Mn	0.029	1.2	1.0
Mn	0.292	0.9	0.6
Mn	0.627	0.2	−0.1
Mn	0.798	•••	−0.2

[a] From Eq. (6) with $a = 100$ and $b = 50$ kG/μ_B.

these are fed into the model phenomenologically, then the temperature dependence of the moment deviations is described reasonably well. This suggests that the moment on an Fe atom depends on its local environment in two ways. There is a dependence on the chemical environment as indicated by the low-temperature moment disturbance and also a dependence on the magnetic environment as indicated by the temperature effects. The dependence on chemical environment is usually attributed to charge screening. Because of the large local moments in this system, we expect that the dependence on magnetic environment is best described in terms of nearest-neighbor exchange.

ACKNOWLEDGMENTS

The authors would like to express their appreciation to S. W. Lovesey for suggesting this problem and for numerous discussions throughout the experiments and to J. L. Sellers for his aid in conducting the experiments.

---

*Research sponsored by the U. S. Energy Research and Development Administration under contract with Union Carbide Corporation.

[1]Y. Koi, A. Tsujimura, and T. Hihara, J. Phys. Soc. Jpn. 19, 1493 (1964).
[2]V. Jaccarino, L. R. Walker, and G. K. Wertheim, Phys. Rev. Lett. 13, 752 (1964).
[3]G. G. Low, Phys. Lett. 21, 497 (1966).
[4]D. A. Shirley, S. S. Rosenblum, and E. Matthias, Phys. Rev. 170, 363 (1968).
[5]S. W. Lovesey and W. Marshall, Proc. Phys. Soc. Lond. 89, 613 (1966).
[6]S. W. Lovesey, Proc. Phys. Soc. Lond. 89, 625 (1966).
[7]S. W. Lovesey, Proc. Phys. Soc. Lond. 89, 893 (1966).
[8]T. Wolfram and W. Hall, Phys. Rev. 143, 284 (1966).
[9]T. E. Cranshaw, C. E. Johnson, and M. S. Ridout, Phys. Lett. 20, 97 (1966).
[10]P. J. Schurer, G. A. Sawatzky, and F. van der Woude, Phys. Rev. Lett. 27, 586 (1971).
[11]D. J. Kim, H. C. Praddaude, and Brian B. Schwartz, Phys. Rev. Lett. 23, 419 (1969).
[12]D. J. Kim, B. B. Schwartz, and H. C. Praddaude, Phys. Rev. B 7, 205 (1973).
[13]W. Marshall, J. Phys. C 1, 88 (1968).
[14]C. J. Borkowski and M. K. Kopp, Rev. Sci. Instrum. 39, 1515 (1968).
[15]M. W. Stringfellow, J. Phys. C 1, 950 (1968).
[16]M. F. Collins and G. G. Low, Proc. Phys. Soc. Lond. 86, 535 (1965).
[17]T. M. Holden, J. B. Comly and G. G. Low, Proc. Phys. Soc. Lond. 92, 726 (1967).
[18]S. J. M. Stoelinga, A. J. T. Grimberg, R. Gersdorf, and G. DeVries, J. Phys. (Paris) 32, C1-330 (1971).
[19]P. J. Schurer, K. W. Maring, and F. van der Woude, Int. J. Magn. 4, 297 (1973).
[20]C. G. Shull and Y. Yamada, J. Phys. Soc. Jpn. Suppl. 17, B-III, 1 (1962).
[21]I. A. Campbell, Proc. Phys. Soc. Lond. 89, 71 (1966).
[22]M. B. Stearns, Phys. Rev. B 9, 2311 (1974).
[23]I. Vincze and G. Gruner, Phys. Rev. Lett. 28, 178 (1972).